ISSN (Print) : 0974-6846
ISSN (Online) : 0974-5645
Indian Journal of Science and Technology, *Vol 10(13), DOI: 10.17485/ijst/2017/v10i13/103299, April 2017*

Analyzing the Mechanical Properties of Lead Cable used in Cardiac Pacemaker

G. Raja[1*], B. K. Gnanavel[2], T. Ramesh[3] and L. Mahesh Kumar[1]

[1]Department of Mechanical Engineering, St. Peter's University, Chennai – 600054, Tamil Nadu, India; raja.g@drmgrdu.ac.in
[2]Department of Mechanical Engineering, Saveetha Engineering College, Chennai – 602105, Tamil Nadu, India;
[3]Department of Mechanical Engineering, National Institute of Technology, Tiruchirapalli – 620015, Tamil Nadu, India;

Abstract

Objectives: This work investigates the mechanical behaviour of lead cable used in cardiac pacemaker and comparing with theoretical values of equilibrium equations. **Methods/Analysis:** A pacemaker is a medical device which uses electrical impulses to regulate the heartbeat. The lead inside the pacemaker cable fails due to various reasons. One such reason is lead fracture which occurs long after the implantation procedure. The pacemaker is considered as a multi-layered assembly with 1+6+12 helical wires and a straight cylindrical core has been chosen for analysing the mechanical properties which plays an important role in the failure of the lead cable. Any lead cable which is considered as rope has general equations of equilibrium. The mechanical property involves tr and force, strand twisting moment, strand axial strain and contact stress. The same mechanical properties are found by writing programs in MATLAB. **Findings:** The study of mechanical properties of lead cable used in cardiac pacemaker is as same as possible with that of the values checked with the equations of equilibrium and the variations are also less than 2 percentage. **Novelty/ Improvements:** With the change in orientation of helix angle which is always assumed to be constant, is made as 82.53˚/-75.62˚, 73.29˚/62.36˚ and 62.24˚/-71.02˚. This change in orientation has made the better comparison of the mechanical properties of the lead cable used in cardiac pacemaker.

Keywords: Contact Stress, Cable Mechanics, Friction, Strand

1. Introduction

The implantable cardiac pacemaker ensures patients with disorders in heart beat to improve the quality of life by stimulating electrically the heart beat at a suitable rate for the day-to-date activities. For preventing the life threatening situation, the Implantable Cardio-verter Defibrillator (ICD) are accommodated to deliver required levels of electrical impulses to the heart muscle to stop the abnormalities in the heart rhythms and restore the function of the heart. An ICD is a battery operated device placed under the skin in the shoulder that keeps track of heart beat rate.

Leads conduct electric signals for sensing, pacing and defibrillation. Leads are very thin, soft and insulated wires. These leads carry the electrical impulse from the pacemaker to the heart. The construction of lead involves extruded tubes of polymer insulation with one or more wires for conduction purpose. Two or more conductors may be included in a signal lead. The outer diameter of a lead is around 2-3 mm. Cables consisting of tiny individual wire filament of about 0.004 cm in diameter are grouped into strands that are in turn grouped to form the cable. There are three desirable properties for conductors in ICD leads: resistance to fatigue with repetitive stress, corrosion resistance and low electrical

*Author for correspondence

resistivity. MP35N is the primary metal in most cables and coils, a Multiphase (MP) alloy constitute nickel, cobalt, chromium and molybdenum. It was developed for marine application because of its flexion and corrosion resistance but it has relatively high electrical resistivity. In high voltage conduction, to minimize energy loss, MP35N is filled with an efficient such as silver. A tribological studies of material used in the construction of cardiac leads[1,2], the clinical importance of lead wear has been widely studied.

The insulation prevents current from escaping from the conductor into tissue. Silicone elastomer comprises the bulk of all lead bodies. It is a polymer with a siloxane (silicon – oxygen, Si-O-Si) backbone and organic side chains, which is inert, bio-stable, bio-compatible and flexible. It has a high co-efficient of friction and is soft making it prone to implant damage and cold flow ("creep"), increasing deformation under a compressive load, resulting in abrasion failure. There include both external ("Outside-in") abrasions from constant compressive loads and internal ("Inside-out") abrasions from cyclical compression.

The mechanical behaviour of cables has been studied by many researchers since two decades. This cable construction involves a central core and a set of wires in two or three layers wound over the core, which is resulting in an axial pull or tension and the axial twisting moment as the major loads. To extend the cable with greater flexibility, many cables are made of strands to form a cable.

The wire force found in the direction of normal[3] and the contact force along the lateral direction calculated, after evaluating the helix angle in the state of deformation through the equilibrate non-linear equations. Formulation of an exact theory for twisted wire cables[4,5] has some prediction of their effective torsion modulus and estimation of their stiffness. The change in normal and bi-normal curvatures and twist of a helical wire[6] to include the effects of wire stretch based on the generalized strain theories.

The unique formulations with relevant numerical examples[7], which has become a reckoner for the cable and wire rope mechanics. The various analytical slender rod models available for predicting the mechanical behaviour of cables, conductors, wire ropes and helical wire strands and presented with their limitations[8].

In a stranded cable, the types of contacts were explained in detail and a new mathematical model to represent the effect of tangential and normal distributed forces in a combined contact. An analytical model to explain the importance of the interfacial loads and their effects in combined contact and identified the maximum limit at which the contact mode changes from a coupled arrangement of core –wire radial contact. More of Poisson's effects on the wire and the core, the redial contraction of the core due to the contact forces was accounted[9].

2. Materials and Methods

2.1 Equilibrium Equations

A cardiac lead cable consist of a central cylindrical wire used as a core, surrounded by two layer of wires wound in opposite direction. The outer layer of the cable may be made of same or different materials. Depending on the number, the helix angle and the diameter of the wires in any layer and the helix radius of the centre of the wires in that layer, the wires can exhibit a combined contact mode or a radial contact mode.

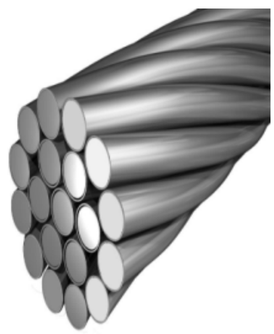

Figure 1. Cardiac lead cable assembly. **Figure 2.** Helically wrapped cable.

Cardiac lead cable assemblies consist of a straight centre core wire surrounded by one or more layers of wires helically wound over it, to form an assembled unit generally called as stranded cables and are used for pacemaker lead. Figure 1 indicates the assembly of a cardiac lead strand. Figure 2 indicates a cable under axial loading and Figure 3 indicates the forces and moments produced on a helical wire, in the normal, bi-normal and axial directions.

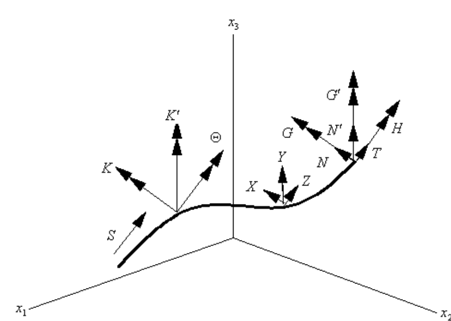

Figure 3. Indicate the forces and moments produced on a helical wire.

The components of the resultant force acting on the cross section of the wire in these directions are indicated by N, N' and T, and the components of the moment resultant are indicated by G, G' and H. X, Y and Z *are* the components of the distributed force developed per unit length of the wire in the above directions and K, K' and Θ are the components of the distributed moment developed per unit length of the wire.

The forces and moments constitute to the equations of equilibrium of the helical wire as derived by Love[3] and are presented as

$$\frac{dN}{ds} - N'\tau_0 + T\kappa_0' + X = 0 \quad (1)$$

$$\frac{dN'}{ds} - T\kappa_0 + N\tau_0 + Y = 0 \quad (2)$$

$$\frac{dT}{ds} - N\kappa'_0 + N'\kappa_0 + Z = 0 \quad (3)$$

$$\frac{dG}{ds} - G'\tau_0 + H\kappa_0' - N' + K = 0 \quad (4)$$

$$\frac{dG'}{ds} - H\kappa_0 + G\tau_0 + N + K' = 0 \quad (5)$$

$$\frac{dH}{ds} - G\kappa_0' + G'\kappa_0 + \Theta = 0 \quad (6)$$

where κ_0 is the normal curvature, κ'_0 is the bi-normal curvature and τ_0 is the twist of the helical wire in the un-deformed state and are respectively expressed in terms of the helix angle α_0 and the helix radius r_0 in the un-deformed state, as under.

$$\kappa_0 = 0 \quad (7)$$

$$\kappa_0' = \frac{\cos^2 \alpha_0}{r_0} \quad (8)$$

$$\tau_0 = \frac{\cos\alpha_0 \sin\alpha_0}{r_0} \quad (9)$$

In a cardiac lead cable assembly, the wires in any layer can maintain combined contact with the wires in the same and adjacent layers, or a pure radial contact in the adjacent layers above[4]. The forces in the above stated contact modes can occur along lines, among wires situated in the same layer and along points or at discrete locations or among wires in the adjoining layers, as the adjacent layers are usually laid with opposite helix pattern arrangement. Such discrete locations are called as trellis contact locations and the contact forces at these locations, though are in the radial direction and are evaluated in similar lines of discussion[10], the derivative terms mentioned in the equilibrium Equations (1) to (6) have been considered in the paper, though many researchers have not accounted them.

2.2 Wire Strains, Curvature Change and Twist

The equations of equilibrium of a helical wire, wire axial strain, wire curvature along the bi-normal direction and the wire twist are defined for a single layer cable assembly[11]. Similar expressions are extended for the cardiac lead cable assembly, with the notation 'i' denoting the wire in the i^{th} layer of the cable.

The change in the helix angle of any wire in the i^{th} layer is arrived from geometry of the strand and is given as under

$$d\alpha_i = \left[\varepsilon - \varepsilon_{\dot{r}} - r_{0i}\tan\alpha_{0i}\left(\frac{d\chi}{h_0}\right)\right]\left(\frac{\tan\alpha_{0i}}{(1-\tan^2\alpha_{0i})}\right) \quad (10)$$

Whereα_{0i} is the helix angle of i^{th} layer helical wire of the cardiac lead cable, ε_{wi} is the axial strain of the i^{th} layer helical wire.

The helix radius for wires in the i^{th} layer before deformation is given by

$$r_{0i} = R_{0c} + 2\sum_{j=2}^{i-1} R_{0\dot{j}w} + R_{0\dot{i}w} \quad (11)$$

The corresponding helix radius in the deformed state is given by the equation

$$r_i = R_{0c}(1-\nu_c\varepsilon) + 2\sum_{j=2}^{i-1} R_{0\dot{j}w}\left(1-\nu_{\dot{j}w}\varepsilon_{\dot{j}w}\right) + R_{0\dot{i}w}\left(1-\nu_{\dot{i}w}\varepsilon_{\dot{i}w}\right) \quad (12)$$

The strand radial strain can be expressed by

$$\varepsilon_{ri} = \frac{r_i - r_{0i}}{r_{0i}} = \frac{dr_i}{r_{0i}} \quad (13)$$

Combining Equations (11), (12) and (13), the radial strain for wires in the i^{th} layer is given as under

$$\varepsilon_{ri} = \frac{-\nu_c R_{0c}\varepsilon - \left(2\sum_{j=2}^{i-1}\nu_{jw} R_{0j}\varepsilon_{jw} + \nu_{iw} R_{0i}\,\varepsilon_{iw}\right)}{r_{0}} \tag{14}$$

Similarly, the axial strain of the wire in the i^{th} layer of a cardiac lead cable is obtained as under

$$\varepsilon_{iw} = \left[\tan^2\alpha_{0i}\varepsilon + \varepsilon_{ri} + r_{0i}\tan\alpha_{0i}\left(\frac{d\chi}{h_0}\right)\right]\cos^2\alpha_{0i} \tag{15}$$

The change in the bi-normal curvature of any wire in the i^{th} layer is obtained from Equation (8) and is given as under

$$d\kappa_i' = -\frac{2\sin\alpha_{0i}\cos\alpha_{0i}}{r_{0i}}d\alpha_i + \frac{\cos^2\alpha_{0i}}{r_{0i}}\varepsilon_{ri} \tag{16}$$

The change in twist of any wire in the i^{th} layer is obtained from Equation (9) and is given as under

$$d\tau_i = \frac{\left(1-2\sin^2\alpha_{0i}\right)}{r_{0i}}d\alpha_i + \frac{\cos\alpha_{0i}\sin\alpha_{0i}}{r_{0i}}\varepsilon_{ri} \tag{17}$$

2.3 Global Cardiac Cable Force And Twisting Moment

Adding the forces and moments of the core, the net strand axial force and the strand axial moment can be expressed as under

$$F=F_c+F_w \tag{18}$$

$$M = M_C + M_W \tag{19}$$

The axial behaviour of above structure shows the coupling between tension and torsion due to the helical design of the wires. Thus, the overall elastic behaviour can be expressed in the form

$$\begin{Bmatrix} F \\ M \end{Bmatrix} = \begin{bmatrix} F_\varepsilon & F_\chi \\ M_\varepsilon & M_\chi \end{bmatrix} \begin{Bmatrix} \varepsilon \\ \frac{d\chi}{h_0} \end{Bmatrix} \tag{20}$$

Where F_ε, F_χ, M_ε and M_χ are the stiffness coefficients of the strand.

Depending on the end conditions of the strand, the above strand force and the twisting moment can be appropriately expressed. In the case of fixed ends, i.e., the angle of twist per unit length of the strand is zero, and in the case of free ends, net twisting moment is zero.

2.4 Modelling Approach

MATLAB is a high level language used for computation of numerical, visualization of image and programming. It can be data analyser, algorithms developer, and models creator and applications. The language and math functions enable to find multiple approaches and reach a solution faster than with spreadsheets or traditional programming languages, such as C/C++ or java. The main feature of the MATLAB software is the interactive environment for exploration of iteration, design and solving the problem.

```
clc
%%Input data
    format long g
      % strand_force= [0 0.010 0.020 0.030 0.040 0.050 0.060 0.070 0.080 0.090 0.100 0.110 0.120 0.130 0.140 0.150]; %in N
    strand_force= [0 0.020 0.040 0.060 0.080 0.100 0.120 0.140 0.150]; %in N
    SF=horzcat (strand_force')
    length=60; %in mm
    total layers=3;
    layer number= [1; 2; 3];
    wiredia= [0.16; 0.16; 0.16];
    lay ratio= [0; 3.98; 7.3];
    lay dir= [1; 1; -1;];
    number of wires= [1; 6; 12];
    youngs modulus= [343000; 343000; 343000];
    poisons ratio= [0.025; 0.025; 0.025];
    cof= [0.05; 0.05; 0.05; 0.05];
  f print f ('\n inner strand geomentry');    LNo_NoW_WD_LR_PR_fc_=horzcat (layernumber', numberofwires', wiredia', layratio', poissonsratio', cof')
```

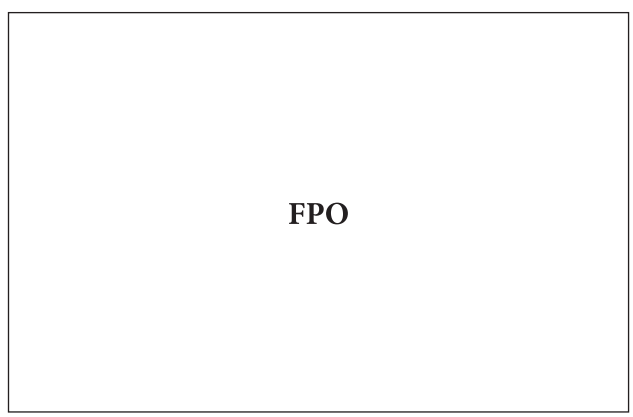

Figure 4. Sample source code to implement the equations using MatLab software.

The strand twisting moment and strand force values are given below in Table 1 and the comparison graph for the values is plotted in Figure 5. The values for Strand Axial Strain and Strand twisting moment are given in Table 2 and the comparison graph plotted in Figure 6. The values for Strand Axial Strain and Contact Stresses are given in Table 3 and the comparison graph plotted in Figure 7

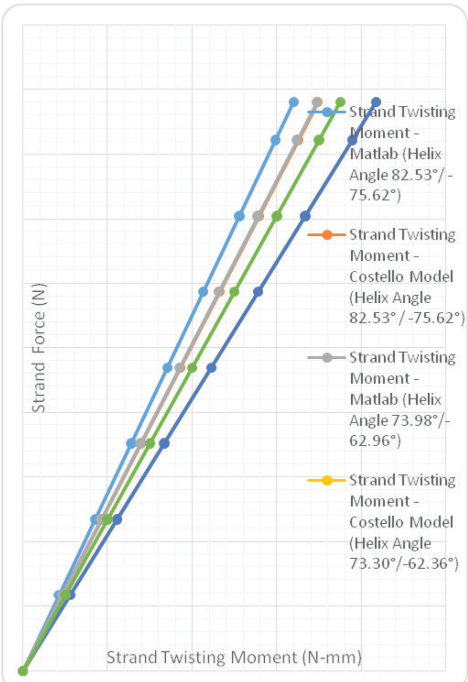

Figure 5. Strand twisting moment vs. strand force.

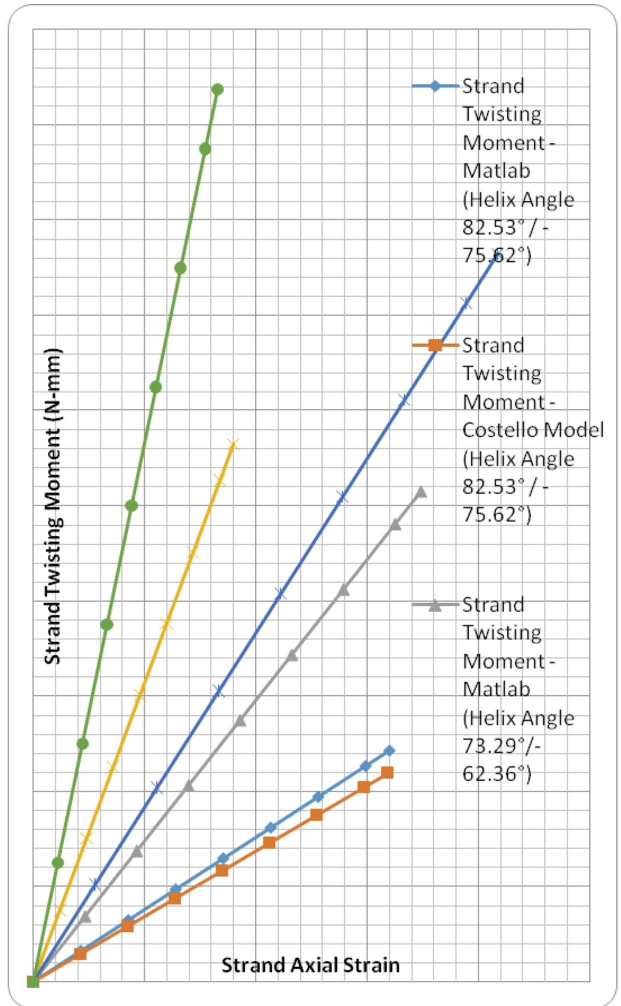

Figure 6. Strand axial strain vs. strand twisting moment.

Table 1. Strand twisting moment and strand force

Strand Force (N)	Strand Twisting Moment - Mat lab (N-mm)	Strand Twisting Moment - Costello Model (N-mm)	Strand Twisting Moment - Mat lab (N-mm)	Strand Twisting Moment - Costello Model (N-mm)	Strand Twisting Moment - Mat lab (N-mm)	Strand Twisting Moment - Costello Model (N-mm)
	Helix Angle (82.53° /-75.62°)		Helix Angle (73.29°/-62.36°)		Helix Angle (62.24°/-71.02°)	
0.0011	4.26E-07	4.24E-07	4.64E-07	4.63E-07	5.56E-07	5E-07
0.0023	8.53E-07	8.47E-07	9.28E-07	9.26E-07	1.11E-06	1E-06
0.0035	1.28E-06	1.27E-06	1.39E-06	1.39E-06	1.67E-06	1.5E-06
0.0046	1.71E-06	1.69E-06	1.86E-06	1.85E-06	2.22E-06	2E-06
0.0058	2.13E-06	2.12E-06	2.32E-06	2.32E-06	2.78E-06	2.5E-06
0.0070	2.56E-06	2.54E-06	2.79E-06	2.78E-06	3.33E-06	3E-06
0.0082	2.98E-06	2.97E-06	3.25E-06	3.24E-06	3.89E-06	3.5E-06
0.0088	3.20E-06	3.18E-06	3.48E-06	3.47E-06	4.17E-06	3.8E-06

Table 2. Strand axial strain and strand twisting moment

Strand Axial Strain	Strand Twisting Moment - Matlab (N-mm)	Strand Twisting Moment - Costello Model (N-mm)	Strand Twisting Moment - Matlab (N-mm)	Strand Twisting Moment - Costello Model (N-mm)	Strand Twisting Moment – Matlab (N-mm)	Strand Twisting Moment - Costello Model (N-mm)
	Helix Angle (82.53°/-75.62°)		Helix Angle (73.29°/-62.36°)		Helix Angle (62.24°/-71.02°)	
4.2E-07	4.6E-07	2.39E-07	5.56E-07	2.20E-07	0.0003	0.0002
8.4E-07	9.2E-07	4.79E-07	1.11E-06	4.41E-07	0.0006	0.0005
1.2E-06	1.3E-06	7.18E-07	1.67E-06	6.61E-07	0.0009	0.0008
1.6E-06	1.8E-06	9.57E-07	2.22E-06	8.81E-07	0.0012	0.0011
2.1E-06	2.3E-06	1.20E-06	2.78E-06	1.10E-06	0.0016	0.0014
2.5E-06	2.7E-06	1.44E-06	3.33E-06	1.32E-06	0.0019	0.0017
2.9E-06	3.2E-06	1.68E-06	3.89E-06	1.54E-06	0.0022	0.0020
3.1E-06	3.4E-06	1.79E-06	4.17E-06	1.65E-06	0.0024	0.0021

Table 3. Contact stress and strand axial strain

Contact Stress (MPa)	Strand Axial Strain - Matlab	Strand Axial Strain -Costello Model	Strand Axial Strain - Matlab	Strand Axial Strain -Costello Model	Strand Axial Strain - Matlab	Strand Axial Strain - Costello Model
	Helix Angle (82.53° /-75.62°)		Helix Angle (73.29°/-62.36°)		Helix Angle (62.24°/-71.02°)	
0	0	0	0	0	0	0
231.98	4.26E-07	4.24E-07	4.64E-07	2.39E-07	5.56E-07	2.20E-07
328.07	8.53E-07	8.47E-07	9.28E-07	4.79E-07	1.11E-06	4.41E-07
401.81	1.28E-06	1.27E-06	1.39E-06	7.18E-07	1.67E-06	6.61E-07
463.97	1.71E-06	1.69E-06	1.86E-06	9.57E-07	2.22E-06	8.81E-07
518.73	2.13E-06	2.12E-06	2.32E-06	1.20E-06	2.78E-06	1.10E-06
568.24	2.56E-06	2.54E-06	2.79E-06	1.44E-06	3.33E-06	1.32E-06
613.77	2.98E-06	2.97E-06	3.25E-06	1.68E-06	3.89E-06	1.54E-06

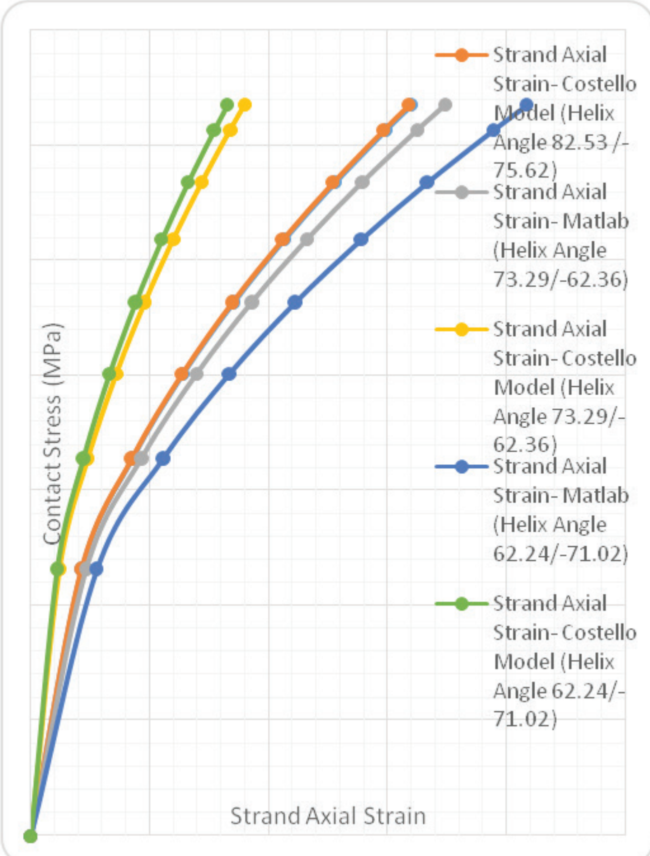

Figure 7. Contact stress vs. strand axial strain.

3. Results and Discussions

All the wires in the layers maintain combined contact mode arrangement. The helical wires maintain line contact with the centre straight wire. To explain the implication of the present model, the comparisons are made for all the stages explained in MATLAB software as follow: Contraction of the helical wires due to Poisson's effects and sliding due to friction, at the contact interfaces are considered.

4. Conclusion

Analytical expressions to examine the prevailing geometry and to identify the proper contact mode during extension of a strand are derived with due consideration of Poisson's effects on the wires, the core and its effects on the geometry of the wire and hence for the revised contact mode using MATLAB. The cable changes its contact mode at critical stress levels from one form to the other have been evaluated. The axial and the torsional response of the cables are evaluated under the prevailing contact modes for cardiac lead cables. Consideration of frictional effects at the contact interfaces, redefined expressions for wire bending and twisting by adopting generalised strain theory and Poisson's effects and its inclusion in the bending, twisting and contact forces are studied.

5. Suggestions for Future Work

The axial response of cardiac lead cable assemblies is studied in this paper, under displacement condition. Extension of the present model to consider the effects of impact in the cardiac lead cable is future concern. Understanding the suitable modelling of the fatigue phenomena of wires at their contact interfaces is of prime importance to predict the wire breakages or wear pattern.

6. References

1. Xiang L, Wang HY, Chen Y, Guan YJ, Wang YL, Dai LH. Modeling of multi-strand wire ropes subjected to axial tension and torsion loads. International Journal of Solids and Structures. 2015 Apr; 58:233–46. Crossref
2. Wang XY, Meng XB, Wang JX, Sun YH, Gao K. Mathematical modeling and geometric analysis for wire rope strands. Applied Mathematical Modelling. 2015 Feb; 39(3–4):1019–32. Crossref
3. Love AEH. A treatise on the mathematical theory of elasticity. 4th edition. Dover Publishers, New York; 1944.
4. Costello GA, Philips JW. A more exact theory for twisted wire cables. Journal of Engineering Mechanics. 1974; 100(5):1096–99.
5. Costello GA, Phillips JW. Effective modulus of twisted wire cables. Journal of Engineering Mechanics. 1976; 102(1):171–81.
6. Ramsey H. Analysis of interwire friction in multi-layered cable under uniform extension and twisting. International Journal of Mechanical Sciences. 1990; 32(8):709–16. Crossref
7. Costello A. Theory of wire rope. Mechanical Engineering Series, Springer Verlag, New York, Berlin Heidelberg; 1997. p. XV,123.
8. Cardou A, Jolicoeur C. Mechanical models of helical strands. Applied Mechanics Reviews. 1997 Jan 1; 50(1):1–14. Crossref

9. Gnanavel BK, Gopinath D, Parthasarathy NS. Effect of friction on coupled contact in a twisted wire cable. International Journal of Applied Mechanics. 2009; 77(2):1–6.
10. Gnanavel BK, Parthasarathy NS. Effect of interfacial contact forces in radial contact wire strand. Archive of Applied Mechanics. 2011 Mar; 81(3):303–17. Crossref
11. Gnanavel BK, Parthasarathy NS. Effect of interfacial contact forces in lateral contact wire strand. In the Proceedings of the World Congress on Engineering, London, UK. 2011; 3:1–7.